Encapsulation Mechanism of Molecular Nanocarriers Based on Unimolecular Micelle Forming Dendritic Core−Shell Structural Polymers

Jianhua Zou, Yongbing Zhao, and Wenfang Shi*

State Key Laboratory of Fire Science and Department of Polymer Science and Engineering, University of Science and Technology of China, Hefei, Anhui 230026, P. R. China

Received: October 6, 2005; In Final Form: December 1, 2005

A series of dendritic core−shell structural polymers with different shell densities were synthesized based on dendritic polyester Boltorn H40 and were demonstrated to form unimolecular micelles in chloroform. The encapsulation mechanism study using Congo red as a guest molecule by fluorescence and UV−vis methods showed that the interaction of Congo red with hydroxyl groups in the dendritic core−shell polymer led to encapsulation. Moreover, the results also indicated that the dendrimer with 43.4% hydroxyl groups end-capped by the long alkyl chains showed the best encapsulation capacity. However, lower and higher alkyl densities both led to lower encapsulation capacities. The former was attributed to the poor compatibility of the polymer with chloroform, and the later was caused by less location sites for the guest molecule inside the core−shell polymer.

Introduction

Unimolecular micelles formed by dendritic core−shell structural polymers have been investigated intensively as molecular nanocarriers, recently.[1−7] In contrast to micelles, which are generally weak physical aggregates of amphiphilic block copolymers in selective solvents,[8−10] unimolecular micelles are stable to various environmental effects, such as dilution, shear force, and pH value and will not burst release the guest molecules out of control. Understanding the reasons for the entrapment of guest molecules and the key factors for encapsulation capacity of unimolecular micelles is important for both academic and application reasons. Surprisingly, to date, most research work has focused on the application of the unimolecular micelles as guest molecular carriers,[1−3] and mechanism study, especially systematic study, is still lacking. Only a few primary mechanisms have been proposed or investigated: the concept of the dendritic box, that guest molecules were captured within the internal cavities of dendritic polymers, was expounded by Jansen;[7] Morgan studied the mechanism by the solvatochromic shift in UV−vis absorbance and ^{1}H NMR analysis;[6] Krämer attributed the encapsulation to the strong interaction of guest molecules with polar groups in the core of dendritic macromolecule, but without experimental demonstration;[5] Pistolis and co-workers located the solubilization sites of guest molecules in dendritic polymers by a fluorescence quenching method.[4]

In this article, a simple approach is employed to investigate the encapsulation mechanism by fluorescence and UV−vis methods, which revealed both the reasons for the entrapment of guest molecules and the key factors that govern the encapsulation capacity of unimolecular micelles. It is supposed that the results will be a theoretical guide for the design of more efficient molecular nanocarriers.

Experimental Section

Materials. Dendritic aliphatic polyester, Boltorn H40 (H40), donated by Perstorp AB, Sweden, was purified according to the literature procedure[11] to give the purified product with a number average molecular weight (M_n) of 6.4×10^3 g/mol and a polydispersity of 1.31. Congo red was purchased from Yuanhang Reagent Co. of Shanghai, China. Both pyridine and *N*,*N*-dimethyl acetamide (DMA) were supplied by First Reagent Co. of Shanghai, China, and were distilled prior to use. 4-(Dimethylamino)pyridine (DMAP) and stearoyl chloride (SC) were purchased from Aldrich. All the reagents, unless specified, were of analytical grade and were used without further purification. Distilled water was used at all times.

Alkylation of H40. A series of core−shell structural polymers with different densities of alkyl chain shell were synthesized. A representative procedure is given as following: H40 (3 g, 26.24 mmol of hydroxyl groups) was dissolved in freshly distilled DMA (20 wt %) in the presence of DMAP (100 mg) and pyridine (3 mL). SC (3.98 g, 13.12 mmol) was then added dropwise to the above H40 solution over a period of 10 min, and the reaction was carried out at 80 °C for 24 h. The product was obtained by three cycles of precipitation by water and filtration and was dissolved in DMA, which was finally purified by dialysis (dialysis tubing, benzoylated cellulose MWCO 1000) in $CHCl_3$, yielding a white fine powder, named a-H40.

Guest Molecule Encapsulation. The compound a-H40 is soluble in a large variety of nonpolar organic solvents (for example, chloroform and dichloromethane) in contrast to H40, which is soluble only in extremely polar solvents, such as DMF, DMA, and pyridine. The transport behavior of the core−shell nanocarrier from a polar solvent to an apolar solvent was tested using Congo red as a guest molecule. Congo red is water soluble anionic dye, which is unsoluble in chloroform. A representative experimental transport procedure is given as following: Congo red aqueous solution (10 mL, 40 μM) was mixed and agitated with an a-H40 chloroform solution (10 mL, 1.0 mg/mL) for 5 min, which will fully load a-H40 with Congo red. After standing and phase separation, the aqueous phase was separated from the chloroform phase for characterization.

Measurements. ^{1}H NMR analysis was carried out on a Bruker AVANCE 300 spectrometer using chloroform-d_1 as a

* To whom correspondence should be addressed. Tel.: +86-551-3606084. Fax: +86-551-3606630. E-mail: wfshi@ustc.edu.

10.1021/jp055694i CCC: $33.50
Published on Web 01/13/2006

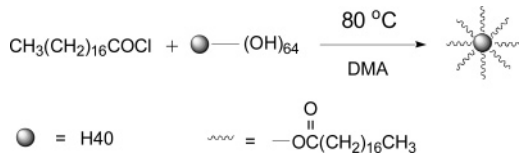

Figure 1. Schematic outline of grafting stearoyl chloride onto H40.

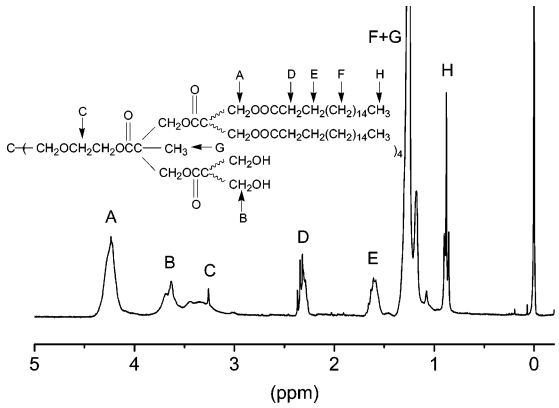

Figure 2. ^{1}H NMR spectrum of H-0.5.

TABLE 1: Characteristics of Amphiphilic a-H40

sample	aver. alkyl arm	alkyl rate[a]	fractional SC converted to arms	M_n (NMR)[b]	M_n (GPC)[c]	M_w/M_n
H-0.1	6.1	9.5%	95.0%	8000	12100	1.51
H-0.3	18.0	28.1%	93.7%	11200	16300	1.43
H-0.5	27.8	43.4%	86.8%	13800	22700	1.45
H-0.7	37.0	57.9%	82.7%	16200	25900	1.39
H-1.0	47.4	74.5%	74.5%	19000	27100	1.36

[a] Percent of H40 hydroxyl groups end-capped by alkyl chains. [b] Calculated based on the ^{1}H NMR data. [c] Measured by GPC with a polystyrene standard.

solvent. The molecular weight and its distribution were determined on a Water 151S gel permeation chromatograph (GPC), using DMF as an eluent. The refractive index increment *(*d*n*/d*C*) of a-H40 in chloroform was determined by an Abbe refractometer and a novel differential refractometer.[12] The UV−vis measurements were carried out using a UV-2410PC (SHIMADZA) instrument. The fluorescence spectra were obtained using a RF-5301PC (SHIMADZA) spectrometer.

Results and Discussion

Alkylation of H40. The schematic outline of grafting an alkyl long chain onto H40 is depicted in Figure 1. A series of core−shell structural polymers were prepared according to different molar ratios of H40 hydroxyl groups to SC of 1:0.1, 1:0.3, 1:0.5, 1:0.7, and 1:1, and they were denominated as H-0.1, H-0.3, H-0.5, H-0.7, and H-1.0, respectively. The percent of hydroxyl groups of H40 reacted with SC was quantified according to the ^{1}H NMR spectrum of a-H40 (Figure 2) by comparing the proton integration of A (δ 4.395−4.140, CH_2OCO) and B (δ 3.773−3.565, CH_2OH), as listed in Table 1. It can be seen that the fraction of SC converted into the shell of the polymer decreases gradually from H-0.1 to H-1.0. For H-1.0, only 74.5% of SC was grafted to H40. The steric hindrance of hydroxyl groups on the periphery of H40 is the main causation of low conversion. It is considered that the overall shape of the dendritic polymer exhibits a structural change from a very open, domed, and loose structure at low generation to a more dense, spheroid-like topology at high generations,[13] that is the terminal groups are more concentrated on the periphery.[14,15] Therefore, for H40 theoretically having 64 hydroxyl groups on the periphery, the steric hindrance for further alkyl chain grafting becomes high.[16,17] The molecular weight and its distribution of a-H40 by the GPC method are also listed in Table 1, indicating the successful synthesis.

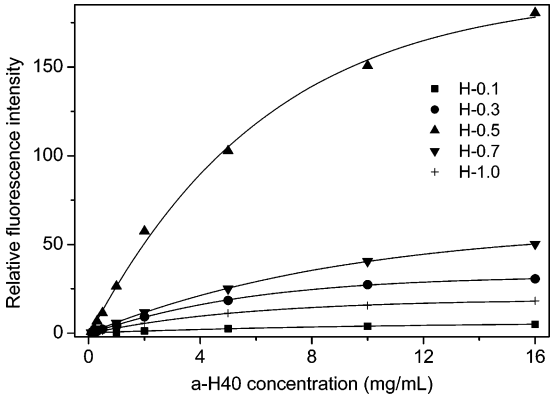

Figure 3. Relative fluorescence intensity of excitation spectra at 324 nm as a function of the concentration of a-H40.

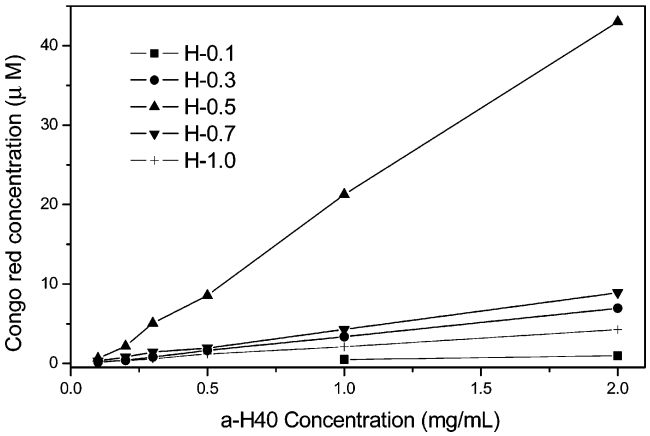

Figure 4. Encapsulation capacity of a-H40 at different concentrations.

Unimolecular Micelle Behavior in Chloroform. The encapsulation capacity of a-H40 was characterized by the fluorescence measurement. The chloroform solutions of a-H40 with different concentrations were mixed with a Congo red aqueous solution. The reduced excitation fluorescence intensity of the aqueous phase at 324 nm was plotted against the a-H40 concentration, as shown in Figure 3. It can be seen that H-0.5 shows the highest encapsulation capacity, whereas the lower and higher degrees of alkylation both result in lower encapsulation capacities. This result is consistent with the degree of alkylation for the efficient transport (40−45%) obtained by other researchers.[5,18] It can also be observed that the encapsulated Congo red decreases gradually with the decrease in the polymer concentration. This is very different from typical S-shaped curves formed by surfactants, of which the encapsulation capacity decreases sharply at their critical micelle concentrations.[21,22] The result reveals that no association occurs between a-H40 molecules, which might exist as unimolecular micelles in chloroform.

To gain quantitative information about the encapsulation capacity of a-H40, the fluorescence intensities in Figure 3 are converted into concentrations, as shown in Figure 4, according to the fluorescence intensity−concentration standard curves (see the Supporting Information). It can be seen that, except for H-0.1 showing no encapsulation capacity at low concentration, the Congo red concentration increases with increasing concentration of a-H40 in a nearly linear manner when the concentration of

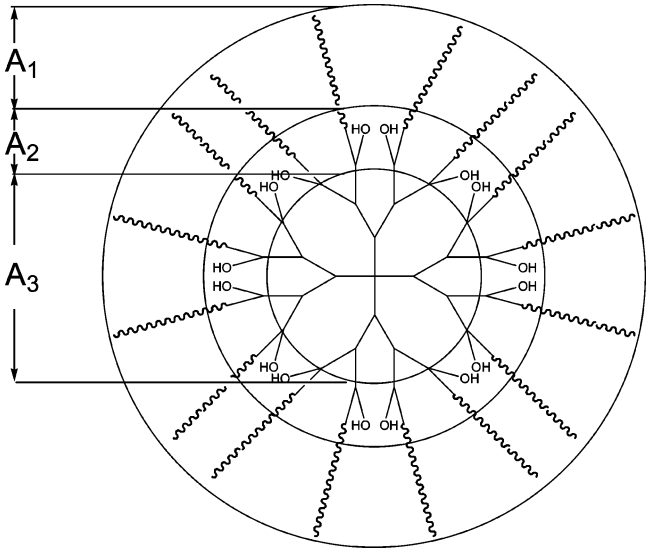

Figure 5. Schematic drawing for the division of the a-H40 molecular structure into three parts.

a-H40 is below 2.0 mg/mL, which indicates a-H40 molecules behaving as unimolecular micelles in chloroform.[20,23] However, when the concentration of a-H40 is beyond 2.0 mg/mL, the encapsulated Congo red does not increase linearly with the a-H40 concentration, revealing the formation of aggregates in chloroform[23] (see the Supporting Information).

Laser lighting scattering (LLS) experiments were carried out to clarify whether a-H40 were present as unimolecular micelles in chloroform, since the theoretically estimated diameter of a-H40 is approximately 8 nm (see the Supporting Information), which is below the detection limit (10 nm) of the LLS used in the study. The static LLS experiments for all a-H40 samples in the concentration range of 0.1−2.0 mg/mL showed no scattering intensity at any angle, whereas scattering intensity was observed when the concentration was over 2.0 mg/mL. Therefore, in the concentration range of 0.1−2.0 mg/mL, a-H40 samples were present as unimolecular micelles in chloroform, whereas aggregates were formed over the concentration boundry. The results are consistent with that observed from the above fluorescence measurements.

Encapsulation Mechanism. *Reason for the Entrapment of Guest Molecules.* It has been demonstrated that Congo red can be trapped in the unimolecular micelles formed by a-H40 in chloroform at a proper concentration. To investigate why the guest molecules can be trapped by unimolecular micelles, the following consideration is taken. First, the a-H40 molecular structure is divided into three parts with different physiochemical properties, as shown in Figure 5, denoted as A_1, A_2, and A_3, respectively. A_1 is the long alkyl chain shell with an apolar microenvironment; A_2 represents the junction area of the shell with the H40 core, where polar hydroxyl groups are located; A_3 is the core with repeating ester units. Second, chloroform, methanol, and ethyl acetate were selected to physicochemically mimic the microenvironment of A_1, A_2, and A_3, respectively. Chloroform was selected due to its good solubility for alkyl chains. It is supposed that Congo red molecules would be most likely surrounded by chloroform molecules if they are located in A_1.

It has been extensively studied that the fluorescence emission and excitation spectra of some molecular probes, such as pyrene, are sensitive to the polarity of the surrounding microenvironment. Moreover, the excitation spectra always exhibit a blue-shift when the polarity of the environment increases.[24] The

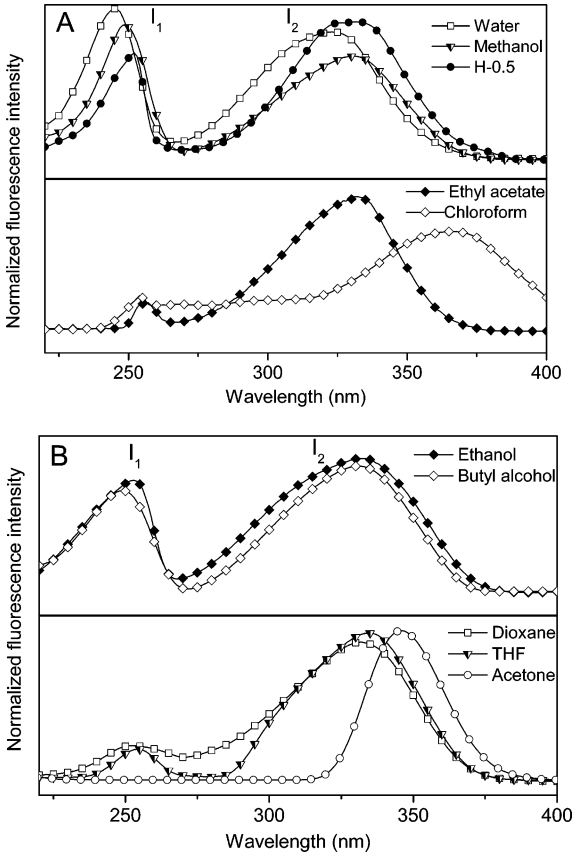

Figure 6. Fluorescence excitation spectra of Congo red in H-0.5 and different solvents.

excitation spectra of Congo red in H-0.5 and mimic solvents are depicted in Figure 6A. Taking the excitation spectrum of Congo red in water as a standard, its spectrum in H-0.5 shows almost the same red-shift as those in methanol and ethyl acetate. However, the red-shift is more distinct for chloroform, which indicates that an interaction between Congo red and A_1 should not take place. Consequently, Congo red molecules are not located in A_1. Despite the displacement of spectra, it is clear that all the fluorescence spectrum traces fall into two distinct groups, of which the overall shapes show the difference in the ratio of fluorescence intensity between I_1 and I_2 (I_1 and I_2 are indicated in Figure 6). The I_1/I_2 values are calculated to be 1.18, 1.292, and 0.781 for Congo red in water, methanol, and H-0.5, respectively, whereas only 0.22 for ethyl acetate and 0.36 for chloroform. From the same characteristic for water, methanol, and H-0.5 of bearing hydroxyl groups, it is inferred that the high I_1/I_2 value might result from the interaction of Congo red molecules with hydroxyl groups. The inference was confirmed by the excitation spectra of Congo red in ethanol, butyl alcohol, acetone, THF, and dioxane (Figure 6B), showing the I_1/I_2 values of 0.838, 0.805, 0, 0.211, and 0.241, respectively. The I_1/I_2 value of 0.781 for H-0.5 approximates to the value for butyl alcohol but is much higher than those for solvents that bear no hydroxyl groups, indicating that the interaction takes place between Congo red molecules and hydroxyl groups of H-0.5. Consequently, the conclusion can be drawn that the interaction of guest molecules with hydroxyl groups in the dendritic core−shell structural polymers is the main reason leading to the encapsulation and that the hydroxyl groups act as anchors for guest molecules to be located. Therefore, Congo red molecules are located in the A_2 region.

To further confirm the results obtained from fluorescence measurements, UV−vis measurements were carried out. It has

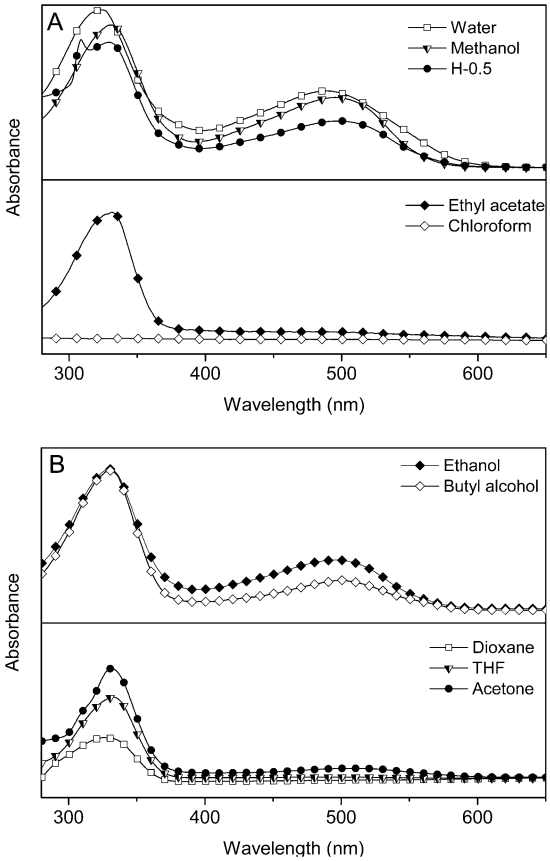

Figure 7. UV−vis absorbance spectra of Congo red in H-0.5 and different solvents.

been demonstrated that the UV−vis spectrum of a solvatochromic dye showed a red-shift as the solvent polarity decreased.[6] As shown in Figure 7A, the UV−vis spectrum of Congo red in water shows a λ_{max} at 324 nm, while the λ_{max} in methanol, ethyl acetate, and H-0.5 are all at 331 nm. This indicates that methanol, ethyl acetate, and H-0.5 show almost the same polarity for Congro red, which is lower than that of water. However, from the spectra in methanol and H-0.5, a strong absorbance at 495 nm is observed, while only a very weak absorbance is discovered at around this wavelength for ethyl acetate. From the UV−vis spectra of Congo red in ethanol, butyl alcohol, acetone, THF, and dioxane (Figure 7B), it is further demonstrated that the absorbance at around 495 nm is attributed to the interaction of Congo red molecules with hydroxyl groups. Therefore, the spectrum of Congo red entrapped by H-0.5, which shows a strong absorbance at 495 nm, reveals the interaction of Congo red molecules with hydroxyl groups of H-0.5. The same conclusions can be drawn that the interaction of Congo red molecules with hydroxyl groups of a-H40 leads to encapsulation and that Congo red molecules are located in A_2. The absorbance spectrum of Congo red in a chloroform solution was also measured and showed almost no absorbance, which is attributed to the poor solubility of Congo red in chloroform.

Factors Affecting Encapsulation Capacity. It has been shown that H-0.5 with 43.4% hydroxyl groups end-capped by long alkyl chains possesses the highest encapsulation capacity, whereas lower and higher alkyl densities both result in low encapsulation capacities. Because hydroxyl groups are considered to be the anchors for guest molecules, it is easy to understand that the encapsulation capacity would decrease when most of the hydroxyl groups were end-capped by alkyl chains. But why does low alkyl density also lead to low encapsulation capacity?

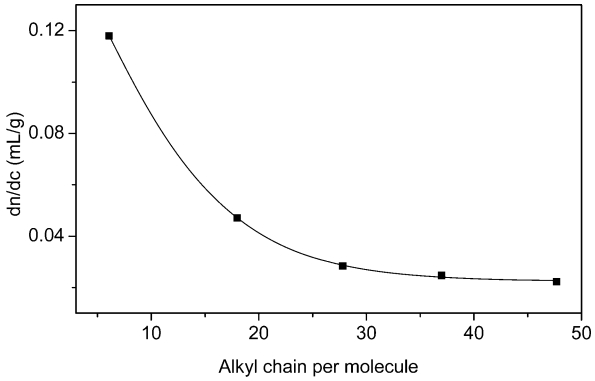

Figure 8. Refraction index increment of a-H40 as a function of the number of alkyl chains per molecule.

It has been found that the refractive index increment (d*n*/d*c*) of a polymer decreases with its increasing compatibility with a solvent.[19] A polymer stretches extensively in a good solvent, leading to more solvent molecules associating with the polymer chains. The d*n*/d*c* of a-H40 in chloroform was measured (detailed information for the d*n*/d*c* determination is given in the Supporting Information), as shown in Figure 8. With the increasing number of alkyl chains grafted onto H40, the d*n*/d*c* value decreases distinctly, indicating that the compatibility of a-H40 with chloroform increases gradually. This is because chloroform is a good solvent for the alkyl shell but is a bad solvent for the H40 core. Therefore, with only a few alkyl chains as the shell, a-H40 shows poor compatibility with chloroform and shrinks into a compact structure, which makes the Congo red molecules difficult to encapsulate inside the microcavities of a-H40, resulting in a low encapsulation capacity.

The conclusion could be drawn that the encapsulation capacity of a-H40 is highly governed by two factors: (1) the content of polar groups in a-H40. More polar groups will anchor more guest molecules into a-H40; (2) its compatibility with the solvent. Better compatibility leads to a higher encapsulation capacity.

Conclusions

Amphiphilic dendritic core−shell structural polymers with different shell densities were synthesized and were demonstrated to form unimolecular micelles in chloroform. Congo red as a guest molecule was encapsulated by the micelles, that, due to its interaction with hydroxyl groups in the polymer and the encapsulation capacity of the unimolecular micelles, was controlled by two factors: one is the number of hydroxyl groups in the polymers, and another is the compatibility of the polymer with the solvent. It is supposed that more efficient molecular nanocarriers will be designed following our results.

Acknowledgment. The financial support of China NKBRSF Project (2001CB409600) and the National Natural Science Foundation of China (50233030) is gratefully acknowledged.

Supporting Information Available: Standard curve of fluorescence intensity versus the concentration of Congo red in aqueous solution, encapsulation capacity of a-H40 at different concentrations, theoretical estimation of the diameter of a-H40, and general procedure to determine the d*n*/d*c* values of dendritic polymers in chloroform. This material is available free of charge via the Internet at http://pubs.acs.org.

References and Notes

(1) Liu, M.; Kono, K.; Fréchet, M. J. *J. Controlled Release* **2000**, *65*, 121.
(2) Sideratou, Z.; Tsiourvas, D.; Paleos, C. M. *Langmuir* **2000**, *16*, 1766.
(3) Sunder, A.; Krämer, M.; Hanselmann, R. *Angew. Chem., Int. Ed.* **1999**, *38*, 3352.
(4) Pistolis, G.; Malliaris, A.; Tsiourvas, D.; Paleos, C. M. *Chem.—Eur. J.* **1999**, *5*, 1440.
(5) Krämer, M.; Stumbé, J.; Türk, H.; Krause, S.; Komp, A.; Delineau, L.; Prokhorova, S.; Kautz, H.; Haag, R. *Angew. Chem., Int. Ed.* **2002**, *41*, 4252.
(6) Morgan, M. T.; Carnahan, M. A.; Immoos, C. E.; Ribeiro, A. A. *J. Am. Chem. Soc.* **2003**, *125*, 15485.
(7) Jansen, J.; Debrabandervandenberg, E.; Meijer, E. *Science* **1994**, *266*, 1226.
(8) Zeng, F.; Liu, J.; Allen, C. *Biomacromolecules* **2004**, *5*, 1810.
(9) Gan, Z.; Jim, T. F.; Li, M.; Zhao, Y.; Wang, S. G.; Wu, C. *Macromolecules* **1999**, *32*, 590.
(10) Zhao, Y.; Hu, T.; Lv, Z.; Wang, S.; Wu, C. *J. Polym. Sci., Part B: Polym. Phys.* **1999**, *37*, 3288.
(11) Ornatska, M.; Peleshanko, S.; Rybak, B.; Holzmueller, J.; Tsukruk, V. *Adv. Mater.* **2004**, *16*, 2206.
(12) Wu, C.; Xia, K. Q. *Rev. Sci. Instrum.* **1994**, *65*, 587.
(13) Naylor, A. M.; Goddard, W. A.; Kiefer, G. E.; Tomalia, D. A. *J. Am. Chem. Soc.* **1989**, *111*, 2339.
(14) Topp, A.; Bauer, B. J.; Klimash, J. W.; Spindler, R.; Tomalia, D. A.; Amis, E. J. *Macromolecules* **1999**, *32*, 7226.
(15) Uppuluri, S.; Keinath, S. E.; Tomalia, D. A.; Dvornic, P. R. *Macromolecules* **1998**, *31*, 4498.
(16) Haba, Y.; Harada, A.; Takagishi, T.; Kono, K. *J. Am. Chem. Soc.* **2004**, *126*, 12760.
(17) Hedden, R. C.; Bauer, B. J. *Macromolecules* **2003**, *36*, 1829.
(18) Stirba, S. E.; Kautz, H.; Frey, H. *J. Am. Chem. Soc.* **2002**, *124*, 9698.
(19) Zhang, G. Z.; Liu, L.; Zhao, Y.; Ning, F. L.; Jiang, M.; Wu, C. *Macromolecules* **2000**, *33*, 6340.
(20) Chen, G. H.; Guan, Z. B. *J. Am. Chem. Soc.* **2004**, *126*, 2662.
(21) Wilhelm, M.; Zhao, C. L.; Wang, Y.; Xu, R.; Winnik, M. A.; Mura, J. L.; Riess, G.; Croucher, M. D. *Macromolecules* **1991**, *24*, 1033.
(22) Tang, Y.; Liu, S. Y.; Armes, S. P.; Billingham, N. C. *Biomacromolecules* **2003**, *4*, 1636.
(23) Liu, H.; Jiang, A.; Gao, J.; Uhrich, K. E. *J. Polym. Sci., Part A: Polym. Chem.* **1999**, *37*, 703.
(24) Kalyanasundaram, K.; Thomas, J. K. *J. Am. Chem. Soc.* **1977**, *99*, 2039.